# The Value of the Dopamine $D_{2/3}$ Receptor Ligand $^{18}$F-Desmethoxyfallypride for the Differentiation of Idiopathic and Nonidiopathic Parkinsonian Syndromes

Christian la Fougère[1], Gabriele Pöpperl[1,2], Johannes Levin[3], Björn Wängler[1], Guido Böning[1], Christopher Uebleis[1], Paul Cumming[1], Peter Bartenstein[1], Kai Bötzel[3], and Klaus Tatsch[1,4]

[1]Department of Nuclear Medicine, University of Munich, Munich, Germany; [2]Department of Nuclear Medicine, Klinikum Stuttgart, Stuttgart, Germany; [3]Department of Neurology, University of Munich, Munich, Germany; and [4]Department of Nuclear Medicine, Municipal Hospital Karlsruhe Inc., Karlsruhe, Germany

We evaluated the utility of the selective dopamine $D_{2/3}$ receptor ligand $^{18}$F-desmethoxyfallypride ($^{18}$F-DMFP) for the differential diagnosis of patients with idiopathic parkinsonian syndrome (IPS) and nonidiopathic parkinsonian syndrome (non-IPS). On the basis of the superior sensitivity of PET, we hypothesized that $^{18}$F-DMFP should have properties for the differential diagnosis of these syndromes superior to what has been reported for the more conventional SPECT procedures. **Methods:** A series of 81 patients with parkinsonism (26 women, 55 men; mean age ± SD, 68 ± 11 y) were included in this retrospective analysis. A 30-min $^{18}$F-DMFP PET recording was acquired starting 1 h after injection of the tracer (180–200 MBq, intravenously). The specific binding (SB) in divisions of the striatum was calculated relative to the occipital cortex using an observer-independent semiautomatic volume-of-interest–based technique. The optimal SB threshold was defined by means of receiver-operating-characteristic analysis, which was also used for the evaluation of the diagnostic performance of SB, ratios between striatal subregions, and absolute asymmetries in SB. **Results:** Significant differences ($P < 0.001$) were found in striatal SB between IPS and non-IPS, most notably in the posterior putamen, for which the diagnostic power for discrimination of IPS and non-IPS was the highest (sensitivity, 87%; specificity, 96%; and accuracy, 91%). A further gain of diagnostic power (sensitivity, 92%; specificity, 96%; and accuracy, 94%) was obtained through discriminant analysis combining 3 parameters: SB of the posterior putamen, the posterior–to–anterior putamen ratio, and the posterior putamen–to–caudate ratio. **Conclusion:** $^{18}$F-DMFP PET is useful for the differential diagnosis of IPS and non-IPS in patients with parkinsonism. The findings are consistent with relative sparing of $D_{2/3}$ receptors in the dopamine-denervated putamen of IPS patients, in contrast to a more substantial loss of striatal dopamine receptors in non-IPS patients. The PET procedure for this differential diagnosis was superior to the reported experience with $^{123}$I-iodobenzamide SPECT.

Parkinsonism refers to a variable complex of symptoms occurring in idiopathic parkinsonian syndrome (IPS) and in several other neurodegenerative syndromes such as multiple-system atrophy, progressive supranuclear palsy, and corticobasal degeneration, which are collectively termed non-IPS (atypical parkinsonian syndromes). Given the different clinical courses of these syndromes, obtaining a timely differential diagnosis is crucial for gaining an accurate prognosis and for optimal management and treatment. However, the early clinical presentations of the several parkinsonian syndromes can be difficult to distinguish. Accurate differential diagnosis not only is important for the management and treatment of individual patients but also must be considered in the design of prospective studies of the efficacy of new treatments intended to slow the progression of IPS (1). In several prospective PET studies, the integrity of the nigrostriatal dopamine pathway in IPS patients has been assessed with L-3,4-dihydroxy-6-$^{18}$F-fluoro-phenyl-alanine (2,3), but its utility for differential diagnosis of non-IPS is poorly documented (4).

The more extensive pathology of non-IPS might predict a greater involvement of postsynaptic markers in the basal ganglia. Indeed, molecular imaging studies with ligands for dopamine $D_{2/3}$ receptors are of proven utility for the early diagnosis of parkinsonian syndromes and for longitudinal studies of disease progression (5). A variety of radioligands has been used for clinical studies of $D_{2/3}$ receptors in IPS, by SPECT (e.g., $^{123}$I-iodobenzamide [$^{123}$I-IBZM] and $^{123}$I-epidepride) and PET (e.g., $^{11}$C-raclopride and $^{11}$C-N-methylspiperone) (6–9). Although the PET technique has

superior properties with respect to image quality and sensitivity, enabling the detection in the brain of radioligands at femtomolar concentrations with a spatial resolution of 3–5 mm (5), ^{123}I-IBZM SPECT has found more widespread clinical routine use, despite its lower sensitivity and resolution. The advantage of ^{123}I-IBZM SPECT is imparted by its more favorable physical half-life (13.2 h), which permits its distribution to distant imaging centers. In contrast, ^{11}C-labeled ligands must be prepared at a local cyclotron or radiochemistry unit because of the brief half-life (20 min). This impediment to the wider use of PET for clinical dopamine receptor studies could be overcome through the use of suitable ^{18}F-labeled radioligands. The ^{18}F half-life (110 min) is sufficiently long to permit distribution from a central radiochemistry site to satellite PET centers without excessive loss of specific activity.

The benzamide antagonist ^{18}F-desmethoxyfallypride (^{18}F-DMFP) has binding properties similar to ^{11}C-raclopride (10) and has been characterized for the assay by PET of dopamine $D_{2/3}$ receptors in the living human brain (11,12). In one of these studies, ^{18}F-DMFP was found to be a sensitive agent for the differential diagnosis of patients with parkinsonism, showing high specificity and positive predictive values for the differential diagnosis of IPS and non-IPS (12), albeit in a relatively small group. In the present prospective study, we aimed to evaluate further the aptness of ^{18}F-DMFP PET for the differential diagnosis of IPS and non-IPS in a series of 81 patients with a clinical diagnosis of parkinsonism. Definitive differential diagnosis of IPS or non-IPS was based on clinical follow-up for 2–3 y. We then performed an observer-independent volume-of-interest (VOI) analysis of the PET images in conjunction with receiver-operating-characteristic (ROC) analysis to define the sensitivity and specificity of the ^{18}F-DMFP PET method post hoc.

## MATERIALS AND METHODS

### Subjects

The study included 81 patients with parkinsonism (26 women, 55 men; mean age ± SD, 67.5 ± 10.5 y; range, 40–91 y), who underwent $D_{2/3}$ receptor imaging with ^{18}F-DMFP PET to differentiate between IPS and non-IPS. The patients had been referred to this examination from local movement disorder clinics, and nigrostriatal degeneration had previously been confirmed by a ^{123}I-FP-CIT SPECT scan (GE Healthcare) according to widely accepted criteria (13). All patients were followed clinically for approximately 2 y after SPECT and PET examinations, at which time the clinical differential diagnoses (IPS vs. non-IPS) were evaluated by clinicians on the basis of observations according to the United Kingdom Parkinson Disease Society Brain Bank Diagnostic Criteria for Parkinson Disease (14) and the second consensus statement on the diagnosis of multiple-system atrophy (15). In particular, the final diagnosis was based on documentation of the response to an apomorphine challenge test or the response to dopamine replacement therapy and follow-up clinical examinations, with special attention to the presence or absence of atypical symptoms such as orthostatic hypotension, cerebellar

signs, eye movement disorders, and spasticity. According to these clinical data, 37 patients had IPS and 44 patients had non-IPS.

### Radiochemistry

^{18}F-DMFP (16) was synthesized using a SynChrom R&D automatic synthesis module (Raytest Isotopenmessgeraete) following a procedure published elsewhere (17), with slight modifications: 3 mg (6.2 μmol) of the precursor 2-methoxy-5-[3-[[(4-methylphenyl)sulfonyl]oxy]propyl]-N-[[1-(2-propenyl)-2-pyrrolidinyl]-methyl]-benzamide (ABX) were dissolved in 550 μL of dry $CH_3CN$ and reacted without further treatment with azeotropically dried K-^{18}F-F/Kryptofix 2.2.2. at 90°C for 20 min. After a cooling period, the reaction mixture was diluted with 1 mL of 1% phosphoric acid and purified by high-performance liquid chromatography (250 × 10 mm, RP8; $CH_3CN$:0.1% phosphoric acid, 25:75; 5 mL/min). The fraction containing the desired product was collected, diluted with 11 mL of 0.6 M phosphate buffer (pH 7.2), and loaded on a 30-mg Oasis HLB cartridge (Waters). The cartridge was then washed with 4 mL of isotonic saline and eluted with 1 mL of ethanol. After dilution with 9 mL of isotonic saline, the product was sterilized by membrane filtration (0.2 μm). The radiochemical yields were 55%−60%, and the specific activity was in all cases greater than 126 GBq/μmol. The volume of ^{18}F-DMFP injected as an ethanol:water mixture (1:9) was 1.5 ± 0.5 mL. For the injected activity of 190 ± 10 MBq of ^{18}F-DMFP, the injected tracer mass for all studies was less than 1 μg. Therefore, it can be assumed that there was no relevant receptor occupation in any of the studies.

### PET Image Acquisition and Analysis

Dopamine agonists and other potentially interfering medications, for example, neuroleptics or metoclopramide, were withdrawn before the ^{18}F-DMFP PET investigation according to their biologic half-life. ^{18}F-DMFP was injected as a slow intravenous bolus, and the patients were seated in a quiet room. After 55 min, the patients reclined in the scanning bed of the ECAT EXACT HR[+] PET tomograph (Siemens/CTI), with their head comfortably immobilized within the aperture, using a foam cushion. The scanner acquired 63 contiguous transaxial planes, simultaneously covering 15.5 cm of the axial field of view. The transaxial and axial resolutions (full width at half maximum) of the PET system were 4.6 and 4.0 mm, respectively, at the center of the field of view, and 4.8 and 5.4 mm, respectively, at a radial offset of 10 cm. The emission recording began at 60 min after the start of the bolus and consisted of 3 frames of 10 min each, acquired in 3-dimensional mode. Finally, a brief transmission scan was obtained using a rotating [68]Ge point source. Images were reconstructed as 128 × 128 matrices of 2 × 2 mm voxels by filtered backprojection using a Hann filter with a cutoff frequency of 0.5 Nyquist and corrected for randoms, dead time, and scatter. Images were then transferred to a workstation (Hermes Medical Solutions). After verification of the absence of important head motion between frames, the 3 frames were summed for further analysis.

The data were semiquantitatively evaluated using a modified version of the Brain Analysis Software (BRASS, version 3.5; Hermes Medical Solutions) and standardized 3-dimensional VOIs. This software has been validated previously for SPECT with ^{123}I-IBZM (18) and ^{123}I-FP-CIT (13). The software automatically performs a multistep registration of individual patient images to an ^{18}F-DMFP template for healthy control subjects (Matthias Schreckenberger, University of Mainz). In brief, the individual images are initially fitted to the template image by means of a principal-axes

technique and the iterative simplex algorithm with 9° of freedom. Next, VOIs defining the left and right striatum were finely adjusted to the individual image by further automatic registrations, using 6° of freedom. The VOIs consisted of entire striatum (STR), caudate nucleus (NC), entire putamen (P), and the anterior and posterior divisions of putamen (PA and PP, respectively), to a total of 5 striatal regions per hemisphere. An additional VOI was defined in the occipital cortex (OCC) of the template image. The accurate placement of each VOI was verified carefully and manually adjusted (drag and drop) when necessary. Mean counts per voxel were calculated for each VOI. To evaluate the diagnostic power of $^{18}$F-DMFP PET scans, the following different parameters were assessed:

- Specific binding (SB) for the entire striatum and its subregions, which was calculated according to the formula:

$$SB = \frac{STR - OCC}{OCC}.$$

- The ratios of putamen to caudate nucleus (P-to-NC ratio = $\frac{SB_P}{SB_{NC}}$), posterior putamen to caudate nucleus (PP-to-NC ratio = $\frac{SB_{PP}}{SB_{NC}}$), and posterior putamen to anterior putamen (PP-to-PA ratio = $\frac{SB_{PP}}{SB_{PA}}$).
- Absolute lateralization index (ALI), an unsigned absolute value of the right-to-left-asymmetry of the SB in each the 5 striatal VOIs, irrespective of the more affected side:

$$ALI = \frac{\left| (SB_{STRright} - SB_{STRleft}) \times 2 \right|}{SB_{STRright} + SB_{STRleft}}.$$

## Statistical Analysis

Statistical analysis was performed with the SPSS software package (version 15; SPSS Inc.). Group comparisons between IPS patients and non-IPS patients were performed using the unpaired $t$ test for parametric data, and Mann–Whitney U rank-sum tests were used for nonparametric data. In addition, the performance of the several methods for the differentiation of IPS and non-IPS was assessed by means of ROC curve analysis. This procedure yielded the sensitivity, specificity, positive and negative predictive values (PPV and NPV, respectively), and accuracy of the different parameters for the separation of IPS and non-IPS patients. The best sensitivity and specificity pair for discrimination according to the gold standard clinical diagnosis was calculated. The corresponding threshold was considered optimal when the sum of paired values for sensitivity and specificity reached the maximum, assuming a cost function slope of 1. Finally, the area under the curve (AUC), with the respective SEs, was assessed to obtain objective measures from the diagnostic power of the individual parameters. In addition, discriminant analysis combining different parameters was performed.

We tested the relationship between subject age and SB for the entire striatum by linear regression for the IPS and non-IPS groups.

## RESULTS

The mean age of the IPS patients ($n = 37$) was 65.9 ± 11.3 y (range, 40–85 y) and that of the non-IPS patient group ($n = 44$) was 68.9 ± 9.8 y (range, 47–91 y) ($P = 0.2$).

The mean $^{18}$F-DMFP SB in the entire striatum, left and right (SB$_{STR}$), in IPS patients was 2.16 ± 0.32 (range, 1.52–2.96), compared with 1.55 ± 0.28 (range, 0.86–2.00) in non-IPS patients ($P < 0.001$). The mean specific $^{18}$F-DMFP SB was likewise significantly higher in all striatal divisions of IPS patients than in non-IPS patients (Table 1; $P < 0.001$). In addition SB$_{AP}$ and SB$_{PP}$ differed statistically significantly in IPS patients ($P < 0.001$) but not in non-IPS patients ($P = 0.1$). Stratification of the IPS group by age (<65 y, $n = 13$; >65 y, $n = 24$) did not reveal any statistically significant difference for the parameters described above (0.600 ≤ $P$ ≤ 0.987). Stratification of the non-IPS group (<65 y, $n = 16$; >65 y, $n = 28$) showed a trend toward higher SB values in the older patients in the putaminal subregions (AP, $P = 0.062$; PP, $P = 0.11$) but not in the caudate nucleus. Figure 1 shows transverse images of the striatal dopamine D$_{2/3}$ receptor binding of $^{18}$F-DMFP in single representative patients with non-IPS (Fig. 1A) and IPS (Fig. 1B).

According to our ROC analysis, the optimal threshold for SB in all divisions of striatum had high diagnostic power, with highest scores in the posterior putamen (SB$_{PP}$, 2.05; sensitivity, 86.5%; specificity, 95.5%; NPV, 89.4%; PPV, 94.1%; and accuracy, 91.4%). The second best results were found for the entire striatum (SB$_{STR}$, 1.86; sensitivity, 86.5%; specificity, 90.9%; NPV, 88.9%; PPV, 88.9%; and accuracy, 88.9%). The capacities for each parameter for the differentiation of IPS and non-IPS are shown in Table 1, and the respective ROC curves are shown in Figure 2A.

We found statistically significant differences for the P-to-NC ratio (IPS, 1.18 ± 0.10; non-IPS, 1.07 ± 0.20; $P < 0.01$), PP-to-NC ratio (IPS, 1.27 ± 0.13; non-IPS, 1.02 ± 0.28; $P < 0.001$), and PP-to-PA ratio (IPS, 1.14 ± 0.09; non-IPS, 0.91 ± 0.18; $P < 0.001$). Among these comparisons, the PP-to-PA ratio had the best discrimination power (PP-to-PA ratio, 1.07; sensitivity, 83.8%; specificity, 81.8%; NPV, 85.7%; PPV, 79.5%; and accuracy, 82.7%) (Table 1; Fig. 2B).

Combination of the most informative parameter—SB$_{PP}$—for those patients within only 1 SD of the optimal SB$_{PP}$ threshold as defined by the ROC analysis with the PP-to-PA ratio slightly increased the sensitivity of $^{18}$F-DMFP PET for the discrimination of IPS from non-IPS but at the expense of specificity, as shown in Table 1.

In non-IPS patients, side-to-side asymmetry was significantly higher in the putamen and its subregions and in the entire striatum ($P < 0.01$) but not in the caudate nucleus. However, the assessment of ALI did not substantially improve discrimination of IPS and non-IPS (Table 1).

In the additional discriminant analysis, the best discriminative power was achieved by combining SB$_{PP}$, PP-to-PA ratio, and PP-to-NC ratio as factors, which yielded identical results for the original grouped cases and for the cross-validated grouped cases (sensitivity, 91.9%; specificity, 95.5%; NPV, 93.3%; PPV, 94.4%; and accuracy, 93.8%) (Table 1).

**TABLE 1.** SB in All Striatal Regions, Ratios, and Absolute Lateralization Indices in Patients with IPS and Non-IPS

| Binding and region | IPS | | Non-IPS | | P | ROC (AUC ± SE) | Sensitivity (%) | Specificity (%) | NPV (%) | PPV (%) | Accuracy (%) |
|---|---|---|---|---|---|---|---|---|---|---|---|
| | Mean ± SD | Range | Mean ± SD | Range | | | | | | | |
| Dopamine $D_{2/3}$–specific binding | | | | | | | | | | | |
| Striatum | 2.16 ± 0.32 | 1.52–2.96 | 1.55 ± 0.28 | 0.86–2.00 | <0.001 | 0.936 ± 0.027 | 86.5 | 90.9 | 88.9 | 88.9 | 88.9 |
| Caudate nucleus | 1.91 ± 0.32 | 1.23–2.66 | 1.48 ± 0.25 | 0.84–1.98 | <0.001 | 0.859 ± 0.041 | 73.0 | 86.4 | 79.2 | 81.8 | 80.2 |
| Putamen | 2.23 ± 0.33 | 1.60–3.04 | 1.57 ± 0.31 | 0.79–2.08 | <0.001 | 0.944 ± 0.024 | 86.5 | 93.2 | 89.1 | 91.4 | 90.1 |
| Anterior putamen | 2.12 ± 0.31 | 1.54–2.97 | 1.62 ± 0.28 | 1.00–2.12 | <0.001 | 0.894 ± 0.036 | 83.8 | 86.4 | 86.4 | 83.8 | 85.2 |
| Posterior putamen | 2.42 ± 0.39 | 1.67–3.31 | 1.49 ± 0.42 | 0.46–2.13 | <0.001 | 0.970 ± 0.016 | 86.5 | 95.5 | 89.4 | 94.1 | 91.4 |
| P-to-NC ratio | 1.18 ± 0.10 | | 1.07 ± 0.20 | | <0.01 | 0.690 ± 0.058 | 81.1 | 47.7 | 75.0 | 56.6 | 63.0 |
| PP-to-NC ratio | 1.27 ± 0.13 | | 1.02 ± 0.28 | | <0.001 | 0.830 ± 0.045 | 81.1 | 75.0 | 82.5 | 73.2 | 77.8 |
| PP-to-PA ratio | 1.14 ± 0.09 | | 0.91 ± 0.18 | | <0.001 | 0.907 ± 0.032 | 83.8 | 81.8 | 85.7 | 79.5 | 82.7 |
| Combination $SB_{PP}$ and PP-to-PA ratio | — | | — | | — | — | 97.3 | 84.1 | 97.4 | 83.7 | 90.1 |
| ALI | | | | | | | | | | | |
| Striatum | 0.05 ± 0.04 | | 0.10 ± 0.10 | | <0.01 | 0.372 ± 0.062 | 45.9 | 43.2 | 48.7 | 40.5 | 44.4 |
| Caudate nucleus | 0.08 ± 0.07 | | 0.10 ± 0.06 | | >0.05 | 0.357 ± 0.063 | 62.2 | 20.5 | 39.1 | 39.7 | 39.5 |
| Anterior putamen | 0.05 ± 0.03 | | 0.10 ± 0.11 | | <0.01 | 0.329 ± 0.059 | 75.7 | 11.4 | 35.7 | 41.8 | 40.7 |
| Posterior putamen | 0.08 ± 0.06 | | 0.17 ± 0.18 | | <0.01 | 0.340 ± 0.060 | 86.5 | 11.4 | 50.0 | 45.1 | 45.7 |
| Discriminant analysis ($SB_{PP}$, PP-to-PA ratio, and PP-to-NC ratio) | — | | — | | — | — | 91.9 | 95.5 | 93.3 | 94.4 | 93.8 |

Level of significance from Student t test (P); AUC with respective SE from ROC analysis; and sensitivity, specificity, NPV, PPV, and accuracy for optimal specific binding threshold are presented.
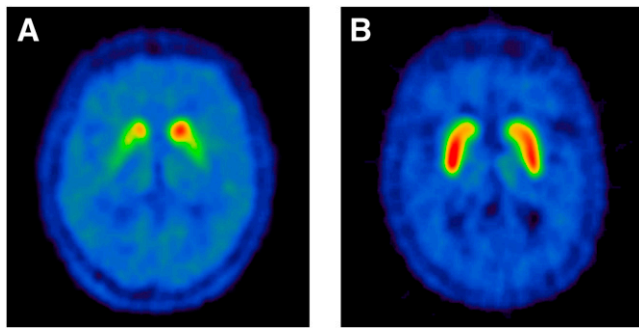
**FIGURE 1.** Striatal dopamine $D_{2/3}$ receptor binding of $^{18}$F-DMFP in 1 patient with non-IPS (A) and 1 patient with IPS (B). Decreased $D_{2/3}$ receptor binding, which was predominant in dorsal part of striatum, is shown in non-IPS (A), whereas increased $D_{2/3}$ receptor binding mainly in posterior putamen could be discerned even visually (B) and was interpreted as relative sparing of $D_{2/3}$ receptor.

## DISCUSSION

Differential diagnosis of parkinsonian syndromes at early disease stages is difficult because of the initial coexpression of signs and symptoms such as asymmetry of motor symptoms, resting tremor, and positive response to L-DOPA treatment. Consequently, non-IPS syndromes can easily be misdiagnosed as IPS (19), and in many cases the true diagnosis emerges late in the disease (20).

We now report that semiquantitative assay of dopamine $D_{2/3}$ receptor with $^{18}$F-DMFP PET provides sensitive discrimination of IPS and non-IPS patients. Several SPECT studies have reported changes in $D_{2/3}$ receptor availability in patients with IPS and non-IPS (12,21–24). With respect to differential diagnosis, it was suggested that patients with IPS had normal or even upregulated $D_{2/3}$ receptor binding, when assessed by means of $^{123}$I-IBZM SPECT (23) or $^{11}$C-raclopride PET (6,25), whereas decreased $D_{2/3}$ receptor availability was found in non-IPS patients (6).

Of the various methods for imaging of dopamine $D_{2/3}$ receptors, $^{123}$I-IBZM SPECT (26) is the most widely used. Although SPECT suffers from well-known limitations in sensitivity and resolution as compared with PET, $^{11}$C-raclopride PET is not available for clinical routine because

of the absolute requirement for an on-site cyclotron-radiochemistry facility. Thus, $^{18}$F-DMFP, compared with $^{11}$C-labeled ligands, lends itself to more routine clinical use while bringing the benefits of persistently high specific activity. $^{18}$F-DMFP has binding properties similar to those of $^{11}$C-raclopride (10), obtaining equilibrium binding within 1 h (17) and possessing a high SB ratio (11). Schreckenberger et al. recently presented an initial comparison of $^{18}$F-DMFP binding in the whole striatum of control subjects and in parkinsonian patients, concluding that this tracer can aid the differential diagnosis of IPS and non-IPS (12). On the basis of this promising result in a group of 35 patients, we wished to make a more detailed regional analysis of $^{18}$F-DMFP PET in an independent population of 81 patients. We hypothesized that $^{18}$F-DMFP binding specifically in the posterior putamen should be especially discriminative, given the more prominent nigrostriatal degeneration in that region (27,28) and particular degeneration of the ventrolateral substantia nigra pars compacta (29), which innervates the posterior putamen (30).

In the present study, we compared several $^{18}$F-DMFP PET indices for the discrimination of IPS and non-IPS. Of these, the SB in the posterior putamen proved to be the best, with 87% sensitivity, 96% specificity, 91% accuracy, and an ROC AUC of 0.97. As such, the $^{18}$F-DMFP binding in the posterior putamen was somewhat better than that in the putamen as a whole. In our hands, $^{18}$F-DMFP binding to the caudate nucleus had the lowest discrimination of the striatal divisions. This stands in contrast to findings of the previous $^{18}$F-DMFP PET study, in which the best discriminative performance was provided by the caudate nucleus, which yielded perfect specificity (100%), albeit with lower sensitivity (74%), accuracy (86%), and AUC (0.86) (12). We also found an AUC of 0.86 in the caudate nucleus, despite the inversion of rank order by striatal region. How do we account for this discrepancy between studies of similar design in cohorts of nearly identical age composition? A key difference arises from the methods used for VOI analysis; whereas we used a 2-step normalization procedure with final manual adjustment, Schreckenberger et al. (12) applied single-slice standard ROIs to the emission image,
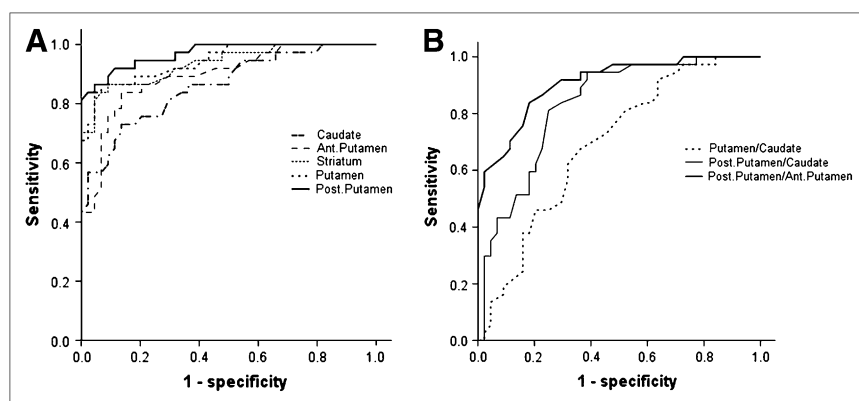


**FIGURE 2.** (A) ROC for SB in caudate nucleus, anterior and posterior putamen, putamen, and striatum. (B) ROC for individual ratios: P to NC, PP to NC, and PP to PA.

without specifying further adjustment of the registration. This resulted in a relative SD for $^{18}$F-DMFP binding in the range of $17\%-26\%$, versus $15\%-20\%$ in our 3-dimensional VOI analysis. The small benefit in precision arising from our method may have favored the putamen VOI for discrimination between the IPS and non-IPS groups.

To search for optimal discrimination between IPS and non-IPS, we also considered the $^{18}$F-DMFP binding ratios within the striatum. The data presented by Schreckenberger et al. yielded mean P-to-NC ratios that were of similar magnitude ($\sim$1.08) in control subjects and the 2 parkinsonian patient groups (12). By similar calculations, we found a comparable P-to-NC ratio for the non-IPS group (1.07) but a significantly higher P-to-NC ratio in our IPS group (1.18). This difference was even more evident in our calculation of the PP-to-NC ratio in the IPS group (1.27), in contrast to the relatively lower ratio seen in our non-IPS group (1.02). Likewise, the PP-to-PA ratio was higher in our IPS patients (1.14) than in our non-IPS group (0.91). These findings suggest relative sparing or upregulation of dopamine $D_{2/3}$ receptors in the putamen, especially in its posterior division, of the IPS patients. Although we have no control material, our contrast of regional $^{18}$F-DMFP binding ratios between IPS and non-IPS patients seems in line with other PET and SPECT studies, which have consistently reported increased putaminal $D_{2/3}$ receptor availability in early IPS patients (31–33). Conversely, the present observations of relative reduction in putaminal $D_{2/3}$ receptor availability in non-IPS are consistent with a previous PET study (21) and with postmortem autoradiographic findings in atypical parkinsonian syndromes (34,35).

In addition to considering absolute measures of $^{18}$F-DMFP binding and ratios, we also investigated the diagnostic power of asymmetry of the $SB_{STR}$, which may be characteristic of neurodegenerative diseases affecting the basal ganglia. As in our earlier report with $^{123}$I-IBZM SPECT (36), we found that the absolute asymmetry of $^{18}$F-DMFP in the striatum was significantly more pronounced in non-IPS than in IPS patients. Nonetheless, this phenomenon is of little value for differential diagnosis. The 2 previous studies from our laboratory using comparable semiquantitative analysis tools reported the diagnostic power of $^{123}$I-IBZM SPECT for the striatum, caudate nucleus, and entire putamen but not for the putaminal subregions, which can scarcely be resolved by SPECT (36,37). These earlier SPECT studies yielded for the whole striatum 87% sensitivity, 73% specificity, and 77% accuracy (36) or 87% sensitivity and 90% specificity (37). Thus, we found still higher diagnostic power for the discrimination between IPS and non-IPS with $^{18}$F-DMFP PET. An independent $^{123}$I-IBZM SPECT study found only 48% sensitivity but 100% specificity and 74% accuracy (38).

In the present study, the magnitude of diagnostic power was increased further by additional discriminant analysis. Even so, $^{18}$F-DMFP PET was not superior to $^{18}$F-FDG PET, for which high diagnostic performance was reported for the diagnosis of progressive supranuclear palsy and multiple-system atrophy ($60\%-85\%$ and $76\%-96\%$ sensitivity and $96\%-99\%$ and $98\%-99\%$ specificity, respectively) (39). $^{18}$F-FDG PET might be especially useful for diagnosing those patients in whom the degenerative process predominantly involves extrastriatal elements of the basal ganglia. The discrimination of non-IPS may also be obtainable from structural MRI (40).

The gold standard for establishing diagnosis in this study was based on diagnostic tests at the time of scanning and clinical follow-up examinations some years later. This may present limitations, given that the definitive diagnosis by histopathologic examination was unavailable. Because the differentiation of several non-IPS syndromes is in itself challenging, we chose to consider the different non-IPS syndromes as a single, albeit heterogeneous, group. Because treatment paradigms are stratified between IPS and the collective of non-IPS disorders, the present approach is operationally useful for clinical purposes.

As in the earlier study by Schreckenberger et al. (12), we found a relatively high prevalence of non-IPS patients (54%) in the entire group, which is nonrepresentative of the typical neurologic clinical setting. This overrepresentation likely results from our recruitment of study patients by referral from specialized movement disorder centers, which would tend to exclude ordinary or uncomplicated IPS cases. Our present lack of a database of control subjects presents limitations, such that we are unable to consider confounders likely presented by the known age-dependent decline of striatal dopamine $D_{2/3}$ receptors. However, we saw no significant differences in mean SB after stratification of the groups by age. Although age must be considered as a nuisance variable, it may be that disease duration or medication history are more important factors in the present study.

## CONCLUSION

$^{18}$F-DMFP PET is an accurate and sensitive tool for the differential diagnosis of IPS and non-IPS in patients. Our semiquantitative assessment of the availability of striatal dopamine $D_{2/3}$ receptors revealed the posterior putamen as the best region for this discrimination. Synopsis with the ratio of binding in the posterior putamen to that in the anterior putamen may be helpful in otherwise inconclusive cases. Greater availability of $D_{2/3}$ receptors in IPS may reveal relative sparing or receptor upregulation due to nigrostriatal degeneration, as compared with a more aggressive disease also affecting the dopamine-receptive neurons. We find the diagnostic power of $^{18}$F-DMFP PET to exceed that of $^{123}$I-IBZM SPECT known from the literature.

## REFERENCES

1. Ravina BM, Fagan SC, Hart RG, et al. Neuroprotective agents for clinical trials in Parkinson's disease: a systematic assessment. *Neurology.* 2003;60:1234–1240.

2. Kumakura Y, Cumming P. PET Studies of cerebral levodopa metabolism: a review of clinical findings and modeling approaches. *Neuroscientist.* 2009; 15:635–650.

3. Whone AL, Moore RY, Piccini PP, Brooks DJ. Plasticity of the nigropallidal pathway in Parkinson's disease. *Ann Neurol.* 2003;53:206–213.

4. Punal-Rioboo J, Serena-Puig A, Varela-Lema L, Alvarez-Paez AM, Ruano-Ravina A. Clinical utility of $^{18}$F-DOPA-PET in movement disorders: a systematic review [in Spanish]. *Rev Esp Med Nucl.* 2009;28:106–113.

5. Brooks DJ. Neuroimaging in Parkinson's disease. *NeuroRx.* 2004;1:243–254.

6. Kaasinen V, Ruottinen HM, Nagren K, Lehikoinen P, Oikonen V, Rinne JO. Upregulation of putaminal dopamine D2 receptors in early Parkinson's disease: a comparative PET study with [$^{11}$C]raclopride and [$^{11}$C]*N*-methylspiperone. *J Nucl Med.* 2000;41:65–70.

7. Tatsch K. Imaging of the dopaminergic system in parkinsonism with SPET. *Nucl Med Commun.* 2001;22:819–827.

8. Farde L, Ehrin E, Eriksson L, et al. Substituted benzamides as ligands for visualization of dopamine receptor binding in the human brain by positron emission tomography. *Proc Natl Acad Sci USA.* 1985;82:3863–3867.

9. Welch MJ, Chi DY, Mathias CJ, Kilbourn MR, Brodack JW, Katzenellenbogen JA. Biodistribution of *N*-alkyl and *N*-fluoroalkyl derivatives of spiroperidol; radiopharmaceuticals for PET studies of dopamine receptors. *Int J Rad Appl Instrum B.* 1986;13:523–526.

10. Mukherjee J, Yang ZY, Brown T, Roemer J, Cooper M. $^{18}$F-desmethoxyfallypride: a fluorine-18 labeled radiotracer with properties similar to carbon-11 raclopride for PET imaging studies of dopamine D2 receptors. *Life Sci.* 1996; 59:669–678.

11. Grunder G, Siessmeier T, Piel M, et al. Quantification of D2-like dopamine receptors in the human brain with $^{18}$F-desmethoxyfallypride. *J Nucl Med.* 2003; 44:109–116.

12. Schreckenberger M, Hagele S, Siessmeier T, et al. The dopamine D2 receptor ligand $^{18}$F-desmethoxyfallypride: an appropriate fluorinated PET tracer for the differential diagnosis of parkinsonism. *Eur J Nucl Med Mol Imaging.* 2004; 31:1128–1135.

13. Koch W, Radau PE, Hamann C, Tatsch K. Clinical testing of an optimized software solution for an automated, observer-independent evaluation of dopamine transporter SPECT studies. *J Nucl Med.* 2005;46:1109–1118.

14. Hughes AJ, Daniel SE, Ben-Shlomo Y, Lees AJ. The accuracy of diagnosis of parkinsonian syndromes in a specialist movement disorder service. *Brain.* 2002; 125:861–870.

15. Gilman S, Wenning GK, Low PA, et al. Second consensus statement on the diagnosis of multiple system atrophy. *Neurology.* 2008;71:670–676.

16. Mukherjee J, Yang ZY, Das MK, Brown T. Fluorinated benzamide neuroleptics. III. Development of (*S*)-*N*-[(1-allyl-2-pyrrolidinyl)methyl]-5-(3-[$^{18}$F]fluoropropyl)-2,3-dimethoxybenzamide as an improved dopamine D-2 receptor tracer. *Nucl Med Biol.* 1995;22:283–296.

17. Siessmeier T, Zhou Y, Buchholz HG, et al. Parametric mapping of binding in human brain of D2 receptor ligands of different affinities. *J Nucl Med.* 2005; 46:964–972.

18. Radau PE, Linke R, Slomka PJ, Tatsch K. Optimization of automated quantification of $^{123}$I-IBZM uptake in the striatum applied to parkinsonism. *J Nucl Med.* 2000;41:220–227.

19. Litvan I. Recent advances in atypical parkinsonian disorders. *Curr Opin Neurol.* 1999;12:441–446.

20. Osaki Y, Wenning GK, Daniel SE, et al. Do published criteria improve clinical diagnostic accuracy in multiple system atrophy? *Neurology.* 2002;59:1486–1491.

21. Ghaemi M, Hilker R, Rudolf J, Sobesky J, Heiss WD. Differentiating multiple system atrophy from Parkinson's disease: contribution of striatal and midbrain MRI volumetry and multi-tracer PET imaging. *J Neurol Neurosurg Psychiatry.* 2002;73:517–523.

22. Tissingh G, Booij J, Winogrodzka A, van Royen EA, Wolters EC. IBZM- and CIT-SPECT of the dopaminergic system in parkinsonism. *J Neural Transm Suppl.* 1997;50:31–37.

23. Schwarz J, Tatsch K, Arnold G, et al. $^{123}$I-iodobenzamide-SPECT predicts dopaminergic responsiveness in patients with de novo parkinsonism. *Neurology.* 1992;42:556–561.

24. Schwarz J, Tatsch K, Arnold G, et al. $^{123}$I-iodobenzamide-SPECT in 83 patients with de novo parkinsonism. *Neurology.* 1993;43(12, suppl 6):S17–S20.

25. Brooks DJ, Ibanez V, Sawle GV, et al. Striatal D2 receptor status in patients with Parkinson's disease, striatonigral degeneration, and progressive supranuclear palsy, measured with $^{11}$C-raclopride and positron emission tomography. *Ann Neurol.* 1992;31:184–192.

26. Kung HF, Pan S, Kung MP, et al. In vitro and in vivo evaluation of [$^{123}$I]IBZM: a potential CNS D-2 dopamine receptor imaging agent. *J Nucl Med.* 1989;30: 88–92.

27. Kish SJ, Shannak K, Hornykiewicz O. Uneven pattern of dopamine loss in the striatum of patients with idiopathic Parkinson's disease: pathophysiologic and clinical implications. *N Engl J Med.* 1988;318:876–880.

28. Jokinen P, Helenius H, Rauhala E, Bruck A, Eskola O, Rinne JO. Simple ratio analysis of $^{18}$F-fluorodopa uptake in striatal subregions separates patients with early Parkinson disease from healthy controls. *J Nucl Med.* 2009;50:893–899.

29. Damier P, Hirsch EC, Agid Y, Graybiel AM. The substantia nigra of the human brain. II. Patterns of loss of dopamine-containing neurons in Parkinson's disease. *Brain.* 1999;122:1437–1448.

30. Fearnley JM, Lees AJ. Ageing and Parkinson's disease: substantia nigra regional selectivity. *Brain.* 1991;114:2283–2301.

31. Antonini A, Schwarz J, Oertel WH, Pogarell O, Leenders KL. Long-term changes of striatal dopamine D2 receptors in patients with Parkinson's disease: a study with positron emission tomography and [$^{11}$C]raclopride. *Mov Disord.* 1997;12:33–38.

32. Ichise M, Kim YJ, Ballinger JR, et al. SPECT imaging of pre- and postsynaptic dopaminergic alterations in L-dopa-untreated PD. *Neurology.* 1999;52:1206–1214.

33. Morrish PK, Sawle GV, Brooks DJ. Clinical and [$^{18}$F] dopa PET findings in early Parkinson's disease. *J Neurol Neurosurg Psychiatry.* 1995;59:597–600.

34. Gonzalez AM, Berciano J, Figols J, Pazos A, Pascual J. Loss of dopamine uptake sites and dopamine D2 receptors in striatonigral degeneration. *Brain Res.* 2000;852:228–232.

35. Pascual J, Berciano J, Grijalba B, et al. Dopamine D1 and D2 receptors in progressive supranuclear palsy: an autoradiographic study. *Ann Neurol.* 1992;32:703–707.

36. Koch W, Hamann C, Radau PE, Tatsch K. Does combined imaging of the pre- and postsynaptic dopaminergic system increase the diagnostic accuracy in the differential diagnosis of parkinsonism? *Eur J Nucl Med Mol Imaging.* 2007;34: 1265–1273.

37. Popperl G, Radau P, Linke R, Hahn K, Tatsch K. Diagnostic performance of a 3-D automated quantification method of dopamine D2 receptor SPECT studies in the differential diagnosis of parkinsonism. *Nucl Med Commun.* 2005;26:39–43.

38. Plotkin M, Amthauer H, Klaffke S, et al. Combined $^{123}$I-FP-CIT and $^{123}$I-IBZM SPECT for the diagnosis of parkinsonian syndromes: study on 72 patients. *J Neural Transm.* 2005;112:677–692.

39. Eckert T, Barnes A, Dhawan V, et al. FDG PET in the differential diagnosis of parkinsonian disorders. *Neuroimage.* 2005;26:912–921.

40. Schrag A, Good CD, Miszkiel K, et al. Differentiation of atypical parkinsonian syndromes with routine MRI. *Neurology.* 2000;54:697–702.